# [3Fe-4S] ↔ [4Fe-4S] cluster interconversion in *Desulfovibrio africanus* ferredoxin III: properties of an Asp¹⁴ → Cys mutant

Johanneke L. H. BUSCH*, Jacques L. BRETON*§, Barry M. BARTLETT†, Fraser A. ARMSTRONG‡, Richard JAMES† and Andrew J. THOMSON*

*School of Chemical Sciences and †School of Biological Sciences, Centre for Metalloprotein Spectroscopy and Biology, University of East Anglia, Norwich NR4 7TJ, and ‡Inorganic Chemistry Laboratory, South Parks Road, Oxford OX1 3QR, U.K.

The 8Fe ferredoxin III from *Desulfovibrio africanus* is a monomeric protein which contains two $[4Fe-4S]^{2+/1+}$ clusters, one of which is labile and can readily and reversibly lose one Fe under oxidative conditions to yield a $[3Fe-4S]^{1+/0}$ cluster. This 4Fe cluster has an $S = 3/2$ ground spin state instead of $S = 1/2$ in the reduced +1 state [George, Armstrong, Hatchikian and Thomson (1989) Biochem. J. **264**, 275–284]. The co-ordination to this cluster is unusual in that an aspartate (Asp¹⁴, D14) is found where a cysteine residue normally occurs. Using a mutant protein obtained from the overexpression in *Escherichia coli* of a synthetic gene in which Asp¹⁴, the putative ligand to the removable Fe, has been changed to Cys, we have studied the cluster interconversion properties of the labile cluster. Analysis by EPR and magnetic-circular-dichroism spectroscopies showed that the Asp¹⁴ → Cys (D14C) mutant contains two $[4Fe-4S]^{2+/1+}$ clusters, both with $S = 1/2$ in the reduced state. Also, unlike in native 8Fe *D. africanus* ferredoxin III, the 4Fe ↔ 3Fe cluster interconversion reaction was found to be sluggish and did not go to completion. It is inferred that the reversibility of the reaction in the native protein is due to the presence of the aspartate residue at position 14 and that this residue might protect the [3Fe-4S] cluster from further degradation.

## INTRODUCTION

Ferredoxins (Fds) are small proteins that contain one or two clusters of the type [2Fe-2S], [3Fe-4S] or [4Fe-4S]. They function as reversible, water-soluble electron carriers in numerous biological processes, including photosynthesis and nitrogen fixation [1,2]. In many bacterial species they apparently carry out a pivotal role in the cytoplasm, accepting electrons from, and distributing electrons to, other proteins in a range of redox-active processes. Some species contain several Fds exhibiting a range of reduction potentials and containing different numbers of clusters. It has been suggested that the ratio of reduced to oxidized Fd may set the effective redox range within the cell. This in turn can control the expression of several energy-transducing enzymes through a redox-sensing protein, as proposed for the SoxR Fe/S protein of *Escherichia coli* [3].

The [3Fe-4S] and [4Fe-4S] clusters have a close structural relationship to one another, in that the [3Fe-4S] cluster differs from the cubane [4Fe-4S] form only by the loss of one iron atom from the corner of the cube [4]. The binding domain of the [4Fe-4S] cluster in Fds is highly conserved throughout evolution and contains the cysteine-rich sequence:

$$Cys^I-Xaa_2-Cys^{II}-Xaa_2-Cys^{III}-Xaa_n-Cys^{IV}-Pro$$

called the 'classic [4Fe-4S] cluster binding motif' or the 'Fd motif' [4]. The 3Fe cluster requires a minimum of three ligands which are usually cysteine residues I, III and IV, whereas a 4Fe cluster usually seems to require four protein ligands to form. In some cases the [3Fe-4S] cluster can reversibly incorporate an additional Fe to form a [4Fe-4S] cluster. However, this type of cluster interconversion is not a property of all proteins that bind a 3Fe cluster, and proteins vary in the ease and rapidity with which metal ion exchange will take place. This reaction may have more widespread occurrence in biology; it may be one of the steps in a regulatory mechanism of activity in the citric-acid-cycle enzyme aconitase [5] and in the iron-responsive element mRNA-binding protein involved in iron homoeostasis [6], as well as in $O_2$ sensing by fumarate nitrate reduction (FNR) protein [7]. The complete set of structural factors which underlie this variation in cluster reactivity is not well understood.

*Desulfovibrio africanus* Fd III (*Da* FdIII) is a 7Fe Fd isolated from the sulphate-reducing bacterium *D. africanus* (Benghazi), which contains one $[3Fe-4S]^{1+/0}$ and one $[4Fe-4S]^{2+/1+}$ cluster per monomer. The monomeric molecular mass of *Da* FdIII is 6585 Da for the 61-amino-acid residue polypeptide. The primary sequence revealed the presence of only seven cysteine residues and, on the basis of spectroscopic similarities with established all-thiolate clusters, it was proposed that they must therefore all be involved in ligation to the two iron–sulphur centres [8,9]. The $[4Fe-4S]^{2+/1+}$ cluster is most probably ligated to the polypeptide chain by the four cysteine residues that form a classic [4Fe-4S]-binding motif, in this case consisting of the triplet Cys⁴¹, Cys⁴⁴, Cys⁴⁷ and the remote Cys²¹ followed by a proline residue (see Scheme 1). The $[3Fe-4S]^{1+/0}$ cluster can hence be co-ordinated only by the three remaining cysteine residues (Cys¹¹, Cys¹⁷ and Cys⁵¹), where Cys^II (residue 14) of the normal motif is replaced by aspartate. In addition to the Cys^II mutation, the proline residue normally found after the remote cysteine residue is a glutamic acid. This double mutation has been observed in only one other case, for the closely related Fd I from *Desulfovibrio vulgaris* (Miyazaki) [10,11]. However the Cys^II → Asp mutation is found in at least three other Fds, from *Pyrococcus furiosus* (*Pf* Fd), *Sulfolobus acidocaldarius* (*Sa* Fd) and *Thermoplasma acidophilum* (*Ta* Fd), which all contain one [3Fe-4S] cluster as isolated [12–14].

---

The [3Fe-4S] cluster of some Fds (*D. gigas* FdII, *Da* FdIII, *Pf* Fd) possesses the interesting property of also displaying incorporation of other metals (M) to form cubane clusters formulated as $[M:3Fe-4S]^{2+/1+}$ [15–19c]. Facile and bi-directional cluster interconversion has been demonstrated in *Da* FdIII using both direct electrochemical methods and spectroscopic studies. Quantitative cluster interconversion as a function of redox level and iron concentration has been demonstrated and values of the equilibrium constants ($K_d$) for dissociation of Fe (and other metals) have been measured ([15,17]; J. N. Butt, J. L. Breton, A. J. Thomson and F. A. Armstrong, unpublished work).

The fourth metal ion cannot be co-ordinated by a thiolate sulphur atom in *Da* FdIII or in *Pf* Fd, and instead an aspartate residue has been proposed to provide the fourth ligand. This is based principally on an NMR study of the 4Fe *Pf* Fd which showed a strongly hyperfine shifted $CH_2$ peak with anti-Curie temperature behaviour for ligand II, which was assigned to Asp[14] [20], and on exogenous ligand binding to the transformed 4Fe cluster in *Da* FdIII [21] and $[M:3Fe-4S]^{2+/1+}$ clusters (M = Fe,Ni or Zn) in *Pf* Fd (J. N. Butt, J. L. Breton, A. J. Thomson and F. A. Armstrong, unpublished work). However, water and/or hydroxy-group co-ordination is also possible, as observed in active aconitase [22].

The ease of interconversion of the [3Fe-4S] cluster thus seems to be related to the presence of a non-thiol ligand in *Da* FdIII, but other factors must be taken into account. For example, *Sa* Fd is a 7Fe Fd as isolated and its [3Fe-4S] cluster does not convert to a 4Fe form, whereas *Dg* FdII has four cysteine ligands and an interconvertible [3Fe-4S] cluster [23].

To improve our understanding of the occurrence of the [3Fe-4S] cluster in Fds and the controlling factors for its conversion into a [4Fe-4S] cluster, we have undertaken a program of site-directed mutagenesis of the 3Fe cluster-binding domain of *Da* FdIII. Recently we reported the heterologous overexpression of *Da* FdIII in *E. coli* using a synthetic gene based upon the published amino acid sequence of *Da* FdIII and using the codon preference for *E. coli* [24]. The resulting recombinant Fd (rec *Da* FdIII) was expressed in *E. coli* in its apo form. Iron–sulphur clusters were subsequently incorporated and the isolated holo-Fd was characterized. We have shown that the electronic and magnetic properties of the two clusters in rec *Da* FdIII are similar to those of the native Fd: the polypeptide co-ordinates a $[3Fe-4S]^{1+/0}$ and a $[4Fe-4S]^{2+/1+}$ cluster and, upon reduction, adventitious Fe(II) can be taken up into the $[3Fe-4S]^0$ cluster to produce a $[4Fe-4S]^{2+/1+}$ cluster.

In the present paper we report the expression of the synthetic gene for the D14C mutant of *Da* FdIII. The D14C *Da* FdIII now contains two Cys$^I$-Xaa$_2$-Cys$^{II}$-Xaa$_2$-Cys$^{III}$-Xaa$_n$-Cys$^{IV}$ domains. The mutated gene was introduced into the same vector as used for recombinant *Da* FdIII and heterologous expression was achieved in *E. coli* host cells. A strategy similar to that developed for rec *Da* FdIII was used for the scaling-up of the expression, purification and reconstitution of this mutant. The electrochemical and spectroscopic characterization of the iron–sulphur clusters of D14C *Da* FdIII is presented.

## EXPERIMENTAL

### Construction of the D14C gene

The synthetic gene for *Da* FdIII, constructed previously [24], was cloned into the M13mp19 phage vector (Pharmacia/LKB) as a 212 bp *Eco*RI–*Hin*dIII fragment. Single-stranded DNA was prepared from the resulting recombinant phage and was then mutagenized using a 21 bp primer whose sequence was complementary to the coding sequence of *Da* FdIII from residue 11 to
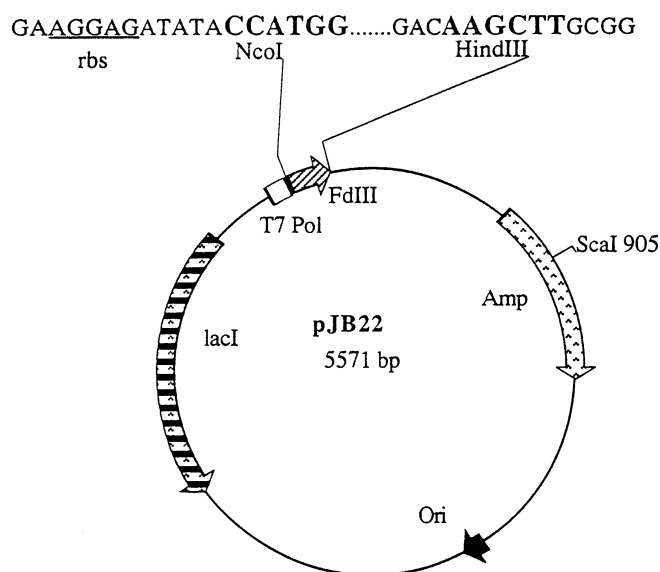


GA**AGGAG**ATATA**CCATGG**.......GAC**AAGCTT**GCGG

**Figure 1    Physical map of the pJB22 expression vector**

The arrows represent the position and direction of transcription of the genes for D14C *Da* FdIII expression (FdIII), ampicillin resistance (Amp), the origin of replication (Ori) and the LacI promoter (LacI). The D14C *Da* FdIII gene is under control of the T7 polymerase promoter (T7 Pol).

17, except that it contained a cysteine codon (TGC) instead of an aspartic acid codon (GAC) at residue 14 (Figure 1). The site-directed-mutagenesis protocol has been described previously [25], and results in a mutagenesis efficiency of greater than 40 %, so that M13 clones containing the mutation can be identified directly by DNA sequencing. The D14C *Da* FdIII gene was then sub-cloned into the expression vector pET21d, using a PCR amplification method [24], resulting in plasmid pJB22.

### Overexpression

*E. coli* strain BL21 (DE3) host cells bearing the plasmid pJB22 were grown at 37 °C on 5 litres of Luria–Bertani medium [26], that was equally divided over ten 2-litre baffled conical flasks and contained 0.7 mM ampicillin (Beecham Research). Expression of the D14C mutant gene of *Da* FdIII was carried out after isopropyl thiogalactopyranoside induction (Melford Laboratories; final concentration 0.8 mM) of the strong T7 promoter in the pET21d vector. Cells were harvested by centrifugation 3 h later.

### Purification and reconstitution

Reagents of at least AnalaR grade were used. Cell paste (65 g) was suspended in 10 mM Tris/HCl buffer (pH 7.6)/5 mM DTT/20 $\mu$M pepstatin/20 $\mu$M leupeptin/2mM PMSF/DNase I (~ 20 $\mu$g; Boehringer), and the suspension was passed twice through a French press (Aminco) at 7 MPa. Unbroken cells (< 10 %) were removed by centrifugation (Sorvall) at 30 000 $g$ for 15 min at 4 °C. Membranes were spun down at 170 000 g for 3.5 h in an ultracentrifuge at 4 °C (Beckmann). The resulting supernatant was subjected to a 30–60 % $(NH_4)_2SO_4$ fractionation. The precipitate was redissolved in 40 mM Tris/HCl (pH 7.6)/5 mM DTT (buffer A) and dialysed overnight (molecular-mass cut-off 3500 Da; Medicell) against buffer A. The dialysed solution was then loaded on to a DE 52 (Whatman) column (diameter 2 cm, length 24 cm) equilibrated with buffer A and chromatographed with a discontinuous NaCl gradient

(0–500 mM). The Fd-containing fractions, identified on SDS/PAGE gels [27], eluted between 150 and 200 mM NaCl. They were concentrated using a 90 % $(NH_4)_2SO_4$ cut, redissolved in 50 mM Tris/HCl (pH 8.3)/5 mM DTT, and dialysed against the same buffer also containing 10 mM EDTA.

This semi-purified Fd fraction (protein concentration 5.5 mg/ml, determined by the Lowry method [28]) contained about 40 % apoFd, as judged by densitometry of SDS/PAGE gels. It was subjected to a reconstitution reaction based upon the procedure developed for rec *Da* FdIII [24]. The reconstitution yields of recombinant *Da* FdIII did not vary significantly over the range of conditions tested [24], therefore the concentration of reagents and incubation times for the bulk reconstitution of the D14C mutant were similar to those used for recombinant *Da* FdIII. The yield in the scaled-up reconstitution reaction of apo-(D14C *Da* FdIII) was about 90 % of reconstituted holo-(D14C *Da* FdIII). Reconstitution and subsequent treatment of the protein took place in an anaerobic glovebox (Faircrest) operating under an $N_2$ atmosphere with $O_2 < 1$ p.p.m.

Bulk reconstitution was carried out with 10 ml of the semi-purified D14C *Da* FdIII fraction, diluted with 50 mM Tris/HCl, pH 8.3, to a total volume of 100 ml, and followed by addition of dithiothreitol (1 M) to a final concentration of 10 mM. The solution was incubated for 5 min before $FeCl_3$ was added to a final concentration of 2 mM. After 15 min incubation, an aliquot of $Na_2S$ was added to give 2 mM final concentration. The reaction mixture was incubated for a further 2 h and then loaded on to a DE 52 (Whatman) column (diameter 3 cm, length 8 cm), equilibrated with buffer A. The column was washed with buffer A and eluted with 450 mM NaCl in buffer A. The brown fraction was diluted to 100 mM NaCl concentration and loaded on to a second DE 52 column (width 1 cm, length 11 cm). This column was developed with a linear gradient from 100 mM to 450 mM NaCl in buffer A, and brown fractions were collected which eluted at 300 mM NaCl.

### Spectroscopy

UV–visible absorption spectra were recorded on a Hitachi U4001 spectrophotometer. Holo-(D14C Fd) concentrations were determined using a molar absorption coefficient ($\epsilon$) of 32 $mM^{-1} \cdot cm^{-1}$ at 386 nm, based on the absorption coefficient of native *Da* FdIII ($\epsilon$ 28.6 $mM^{-1} \cdot cm^{-1}$ at 408 nm) and corrected for 8 Fe per mol.

EPR spectra were recorded on an X-band Bruker ER-200D SRC spectrometer equipped with an Oxford Instruments ESR-900 helium-flow cryostat and a TE-102 cavity. A Hall probe was used to monitor field intensity and a microwave counter (Marconi Instruments, model 2440) was used to measure the microwave frequency. Data were collected using a dedicated Bruker ESP-1600 computer. Spin integrations were performed with a 1 mM Cu(II)/10 mM EDTA solution as standard [29]. Chemical reduction of EPR samples was carried out by addition of microlitre quantities of a concentrated sodium dithionite solution. Procedures for measuring MCD spectra have been described elsewhere [30].

### Direct electrochemistry

The all-glass cell and three-electrode systems used for protein-film voltammetry and bulk solution voltammetry have been described elsewhere [31]. Electrochemical measurements in bulk solution were carried out inside the anaerobic glovebox. The PGE (pyrolytic graphite edge) working electrode was polished prior to each experiment with an aqueous alumina slurry (Buehler micropolish 1.0 $\mu$m) and then sonicated extensively to remove

traces of $Al_2O_3$. The saturated calomel reference electrode (SCE) was maintained at 25 °C, at which temperature we have adopted the correction $E_{0,SCE} = +242$ mV versus the standard hydrogen electrode (SHE). All potentials quoted have been corrected to the SHE scale. Reduction potentials $E_0'$ were determined from the average of oxidative (anodic) and reductive (cathodic) peak potentials, i.e. $(E_{pa} + E_{pc})/2$. Interaction of the protein with the electrode surface was promoted by the addition of small portions of a 0.2 M neomycin sulphate (Sigma) stock solution, to give typically 2 mM final concentration.

## RESULTS

### Purification and reconstitution

SDS/PAGE analysis of cell-free extracts of *E. coli* containing the D14C *Da* FdIII-expressing plasmid pJB22 showed a low-molecular-mass band (indicated by the arrow in Figure 2) that was not present in *E. coli* cells lacking the plasmid. The band mobility was similar to that of recombinant native *Da* FdIII, thus indicating that expression of the mutant Fd had occurred. The expression of apo-(D14C *Da* FdIII) represented ∼ 0.2 % of the total cell proteins, a production level similar to that obtained for recombinant *Da* FdIII [24], which was to be expected, since the same expression system had been used. The heterologous expression in *E. coli* of the D14C mutant produced apoFd only, as no brown fraction, indicative of iron–sulphur clusters, was observed during elution of the cell-free extract on the first DE 52 column. Again this situation is similar to that with recombinant *Da* FdIII, for which no *in vivo* incorporation of iron–sulphur clusters occurred when the synthetic gene was expressed in *E. coli*.

After chemical insertion of the iron-sulphur centres, the purification of holo-(D14C Fd) was achieved using two DE 52 columns. The purity of the most concentrated fractions was checked by PAGE gels and UV–visible spectroscopy. SDS/PAGE showed one single band corresponding to D14C *Da* FdIII (results not shown) with a mobility close to that of *Da* FdI, which has a molecular mass of 7550 Da [32]. The calculated mass of the D14C mutant is 6573 Da. Purified D14C samples were also run on native PAGE and shown not to contain apoFd (Figure 3). This indicated that unchanged apo-Fd was successfully removed in the last purification step and that no degradation of holoFd had occurred during further handling, in contrast with the situation observed for recombinant *Da* FdIII.
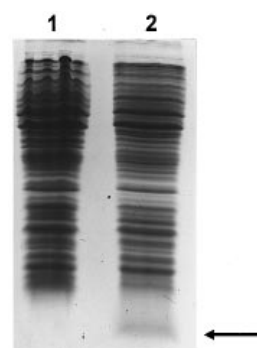
**Figure 2    SDS/PAGE analysis of the expression of D14C *Da* FdIII**

SDS/PAGE gel (20 % acrylamide) was stained with Coomassie Blue. Lane 1, *E. coli* BL21 (DE3) cell-free extract; lane 2, *E. coli* BL21 (DE3) bearing plasmid pJB22 cell-free extract. The arrow indicates the position of D14C *Da* FdIII.

**Figure 3    Native PAGE analysis of D14C *Da* FdIII**

Native PAGE gel (15% acrylamide). Lane 1, *Da* FdI; Lane 2, D14C *Da* FdIII. The gels were stained with Coomassie Blue.
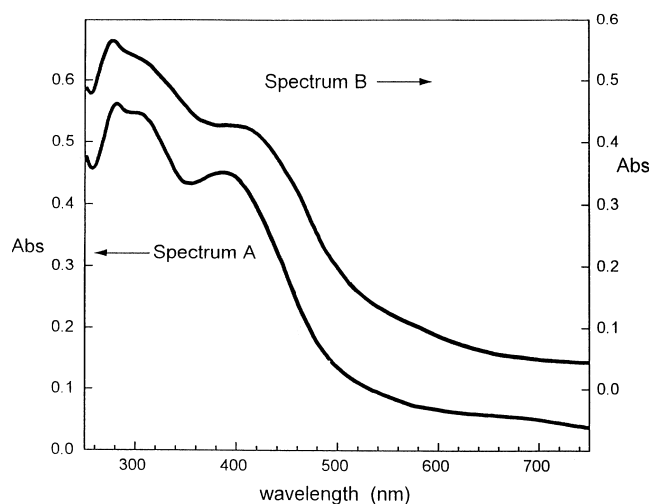


**Figure 4    UV–Visible spectra of (A) D14C *Da* FdIII (lower trace) and (B) native *Da* FdIII (upper trace)**

Trace A: protein concentration, 160 $\mu$M in 40 mM Tris/HCl (pH 7.6)/0.3 M NaCl; pathlength, 1 mm. Trace B: protein concentration, 172 $\mu$M in 0.5 M Tris/HCl, pH 7.4; pathlength, 1 mm.

## Spectroscopy

The UV–visible absorption spectrum of purified D14C *Da* FdIII is shown in Figure 4. The spectrum is rather broad, with band maxima at about 280 nm and 400 nm and a shoulder at 350 nm. The overall shape and intensity of this spectrum compare well with that of native *Da* FdIII [9] (Figure 4). However, the maximum of the broad band around 400 nm, arising from the iron–sulphur chromophores, is shifted to higher energy, from 408 nm for 7Fe native *Da* FdIII to 386 nm for the D14C mutant. This bandshift is also observed in the absorption spectrum of oxidized 8Fe native *Da* FdIII, where the absorption maximum is shifted to 390 nm [15], and is indicative of the presence of [4Fe-4S]$^{2+}$ clusters only. The value of the $A_{386}/A_{280}$ ratio of D14C *Da* FdIII is 0.81, whereas that of native 7Fe *Da* FdIII is 0.76, thus
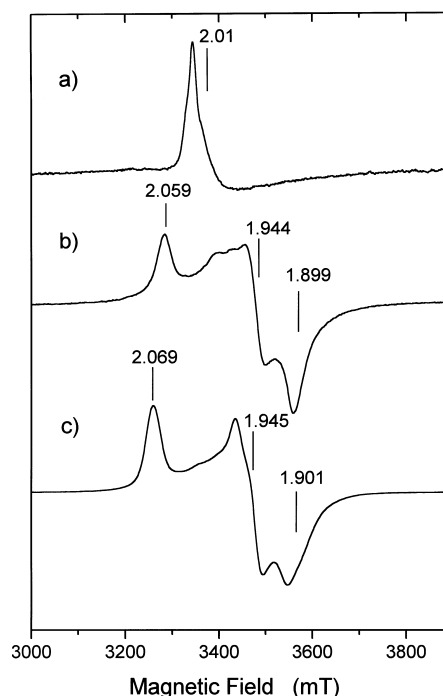


**Figure 5    X-band EPR spectra of (a) oxidized D14C *Da* FdIII, (b) dithionite-reduced D14C *Da* FdIII and (c) dithionite-reduced native *Da* FdIII**

(**a**) Protein concentration, 106 $\mu$M in 40 mM Tris/HCl, pH 7.6; temperature, 8K; gain, $1.6 \times 10^5$. (**b**) Protein concentration, 106 $\mu$M in 40 mM Tris/HCl buffer, pH 7.6; temperature, 19 K; gain, $8.0 \times 10^4$. (**c**) Protein concentration, 611 $\mu$M in 20 mM Tris/HCl buffer, pH 8.6; Temperature, 20 K; gain, $3.2 \times 10^4$. For all spectra microwave power was 2 mW, microwave frequency was 9.40 GHz and modulation amplitude was 1 mT.

indicating an increase in the iron stoichiometry for the D14C mutant.

The X-band EPR spectrum of D14C *Da* FdIII is shown in Figure 5(a). The main feature consists of a small signal at $g = 2.01$. This signal is characteristic of a [3Fe-4S]$^{1+}$ cluster with $S = 1/2$ [33], which is present (1 spin/mol) in the EPR spectrum of oxidized native 7Fe *Da* FdIII. Various samples of oxidized D14C *Da* FdIII were examined and all contained a weak signal at $g = 2.01$. Double integration of the EPR spectrum of several samples gave intensities ranging from 0.10 to $0.15 \pm 0.1$ spin/mol, indicating that the [3Fe-4S]$^{1+}$ cluster is present as a minor component. We could also detect a weak $g = 4.3$ signal at low field (not shown) for most preparations. This resonance is typical of adventitious Fe(III) ions, which could be left over from the reconstitution mixture.

D14C *Da* FdIII was readily reduced by dithionite, as demonstrated by the disappearance in the EPR spectrum of the $g = 2.01$ signal, and the subsequent development of a rhombic signal centred at $g = 1.94$ (Figure 5b). The apparent $g$-values of this signal are $g_1 = 2.059$, $g_2 = 1.944$ and $g_3 = 1.899$. Extra features in the centre of the signal are observed up to a temperature of 25 K, above which the resonance broadens out. The general shape of the spectrum of the reduced sample is unchanged for different buffer systems, although small intensity shifts of the central features appear upon change of buffer. The signal integration yields $1.8 \pm 0.2$ spin/mol, which indicates the presence of two paramagnetic centres per intact Fd. The $g = 1.94$ signal is characteristic of reduced [4Fe-4S]$^{1+}$ clusters with $S = 1/2$. In proteins containing only one such cluster the signal lineshape is usually rhombic, e.g. for the 4Fe Fd *Da* FdI [34]. However, in
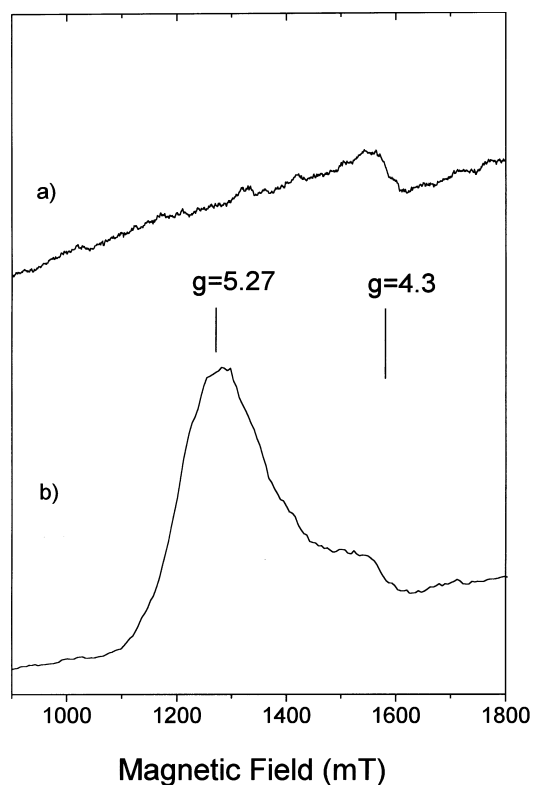
**Figure 6    X-band EPR spectra of dithionite-reduced (a) D14C and (b) wild-type 8Fe *Da* FdIII**

(**a**) Protein concentration, 95 $\mu$M in 20 mM Mes/Hepes/Taps buffer (pH 7.6)/0.1 M NaCl; 10 scans. (**b**) Protein concentration, 611 $\mu$M in 20 mM Tris/HCl buffer, pH 8.6; 1 scan. For both spectra: gain, $1.0 \times 10^5$; temperature, 8 K; microwave power, 80 mW; microwave frequency, 9.40 GHz; and modulation amplitude, 1 mT.



**Figure 7    Low-temperature MCD spectrum of dithionite-reduced D14C *Da* FdIII**

The spectra were recorded at a temperature of 1.6 K, 4.2 K and 10 K at a magnetic field of 5 T. The protein concentration was 404 $\mu$M in 50 mM Hepes/0.1 M NaCl/200 $\mu$M EGTA buffer, pH 7.6, diluted with glycerol (50% v/v). The pathlength was 1 mm.

dicluster (8Fe) Fds, whereas partial reduction of the [4Fe-4S] centres gives a simple rhombic lineshape, additional features often appear on increasing the degree of reduction. These features, which occur principally in the centre of the signal, arise from spin–spin coupling between the two $S = 1/2$ paramagnets [35]. The extra features in the middle of the signal of reduced D14C mutant are therefore likely to arise from intramolecular spin coupling between two [4Fe-4S]$^{1+}$ clusters, which is in agreement with the presence of more than 1 spin/mol of Fd. Comparison of the $g = 1.94$ signal of reduced D14C mutant with that of reduced 8Fe native *Da* FdIII (Figure 5c) shows a similar overall lineshape and small shifts of the $g$-values. However, the extra central features of the D14C mutant signal are not present in the 8Fe native *Da* FdIII EPR signal. The native signal integrates to 1 spin/mol and arises from the [4Fe-4S]$^{1+}$ cluster with $S = 1/2$. This is because the other [4Fe-4S]$^{1+}$ cluster of 8Fe *Da* FdIII, which has a $S = 3/2$ at cryogenic temperatures, has only weak resonances in the $g = 2$ region [15]. Nonetheless, a signal at $g = 5.27$, originating from the ground state $m_s = \pm 3/2$ doublet of this second cluster, is detected in 8Fe *Da* FdIII (Figure 6b). The corresponding region in the EPR spectrum of the D14C mutant clearly lacks any similar resonance (Figure 6a), and only displays a minor feature at a $g$-value of 4.3.

These results imply that the D14C mutant contains two [4Fe-4S]$^{2+/1+}$ clusters, each having a $S = 1/2$ in the reduced $+1$ state. The oxidized $+2$ state is diamagnetic ($S = 0$) and EPR-silent.

To confirm the presence of two [4Fe-4S] clusters in the D14C mutant, a low-temperature MCD spectrum of the dithionite-
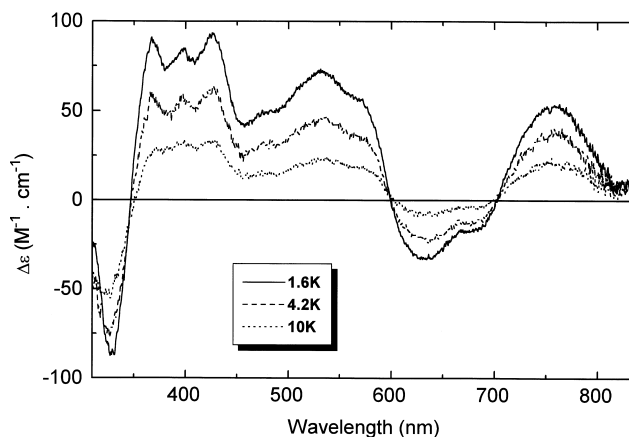
reduced sample was measured (Figure 7). The spectrum is strongly temperature-dependent, which is indicative of the predominant presence of paramagnets [36]. The form of the overall spectrum, notably the MCD bands having a positive sign in the 350–600 nm region and above 700 nm, resembles that of Fds containing [4Fe-4S]$^{1+}$ clusters with $S = 1/2$ [30,36]. The intensity of the MCD spectrum is almost double that expected for one [4Fe-4S]$^{1+}$ cluster. At 1.6 K the maximum amplitude observed is $\approx 70$ M$^{-1} \cdot$cm$^{-1}$ at 550 nm, which compares with a maximum intensity of 40 M$^{-1} \cdot$cm$^{-1}$ for *Da* FdI at the same wavelength ([3Fe-4S]$^0$ clusters have a $\Delta\epsilon < 10$ M$^{-1} \cdot$cm$^{-1}$ at 550 nm) [34]. This result confirms the presence of two [4Fe-4S]$^{1+}$ clusters in D14C *Da* FdIII and the absence of a significant population of [3Fe-4S] clusters. These show a very intense MCD spectrum in the reduced [3Fe-4S]$^0$ state, with intensities up to 250 M$^{-1} \cdot$cm$^{-1}$ in the 400 nm and 700 nm part of the spectrum [30,36].

To test whether either of the 4Fe clusters of D14C *Da* FdIII could be converted readily into a 3Fe form, samples were incubated with potassium ferricyanide. For ferricyanide concentrations between substoichiometric and twice the Fd concentration we observed an increase of the [3Fe-4S]$^{1+}$ cluster population, as judged by the intensity of the '$g = 2.01$' EPR signal, up to $0.6 \pm 0.1$ spin/2 mol of ferricyanide per mol of Fd. Use of a higher concentration of ferricyanide resulted in loss of the [3Fe-4S] cluster and possibly protein denaturation. We could not obtain a preparation having a stoichiometric amount of [3Fe-4S]$^{1+}$ clusters. The reversibility of the reaction was checked by reductive titration with dithionite in the presence of Fe(II) ions, after dialysis of the excess ferricyanide. The resulting sample showed the '$g = 1.94$' EPR signal of the [4Fe-4S]$^{1+}$ cluster, with an intensity corresponding to $\approx 1.8 \pm 0.2$ spin/mol, i.e. similar to that of the starting material.

## Electrochemistry

The cyclic voltammogram of a solution of the D14C mutant is shown in Figure 8. A single cycle displays one set of redox waves with a reduction potential of $-425 \pm 10$ mV at 4 °C (Table 1). This is close to the value of $-400$ mV determined for the 4Fe clusters of *Da* FdIII (couple B) [9,15]. The peak separation of the waves, $\Delta E_p'$ is 105 mV at low scan rates (up to 50 mV·s$^{-1}$) and increases to 150 mV at 500 mV·s$^{-1}$. Plots of $i_{pc}$ and $i_{pa}$, the
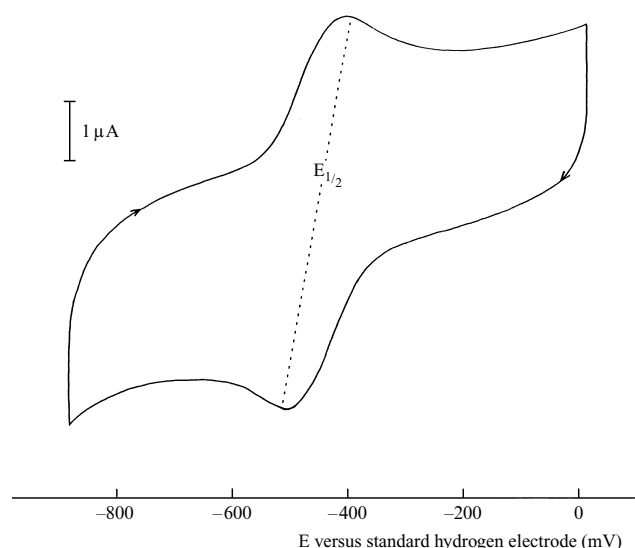
**Figure 8    Bulk solution cyclic voltammogram of D14C *Da* FdIII**

The scan rate was 10 mV·s⁻¹, and the temperature was 4 °C. The protein concentration was 106 $\mu$M in 20 mM Mes/Hepes/Taps/0.1 M NaCl/200 $\mu$M EGTA buffer, pH 7.6, and also contained 2 mM neomycin.

**Table 1    Reduction potentials of the iron–sulphur clusters of native *Da* FdIII and D14C *Da* FdIII**

The values in parentheses refer to adsorbed molecules (in mV versus SHE).

| | $E_0'$ | | |
| --- | --- | --- | --- |
| Fd | [3Fe-4S]$^{1+/0}$ Couple A (A′) | [4Fe-4S]$^{2+/1+}$ Couple B (B′) | [3Fe-4S]$^{0/2-}$ Couple C (C′) |
| Native 7Fe *Da* FdIII† | −140 (−150) | −410 (−393) | −700 |
| 7Fe D14C *Da* FdIII | −125 (−130) | −435 (−450) | − (−690) |
| Native 8Fe *Da* FdIII† | − | −400 (−393)* | − |
| 8Fe D14C *Da* FdIII | − | −425 (−450)* | − |

  * In the 8Fe forms, the two [4Fe—4S]$^{2+/1+}$ couples overlap each other (i.e. couples B + D [17]) and the $E_0'$ value determined is an average of the two couples; D14C data was measured at pH 7.6 (20 mM in Mes/Hepes/Taps/0.1 M NaCl).
  †From references [9,15,18].

cathodic and anodic peak current, versus (scan rate)$^{\frac{1}{2}}$, were linear up to 100 mV·s⁻¹, thus indicating that electron exchange at the PGE electrode is quasi-reversible and diffusion-controlled under these conditions [37]. Because only one set of waves is observed in the cyclic voltammogram of D14C, the two redox couples of the two [4Fe-4S] clusters must lie very close to each other. Also, although the EPR spectrum showed a small proportion of [3Fe-4S] clusters present in the reconstituted fraction, we could not detect any wave at higher potential indicative of 3Fe clusters (couple A in the case of native *Da* FdIII [9]). Upon an increase of protein concentration and change in buffer composition a shoulder appeared on the high-potential side of the oxidation wave, but the origin of this feature is not clear.

Quantitative analysis of the [4Fe-4S] clusters represented by the single redox couple observed by cyclic voltammetry was carried out by exhaustive bulk reduction (−606 mV) and re-oxidation (−206 mV) of solutions of D14C *Da* FdIII. Integration of the total Faradaic current passed gave 1.6±0.2 electrons/mol, thus indicating that wave B corresponds to more than one cluster per mol. However, the number of electrons passed per mol of protein decreased for subsequent reduction/oxidation cycles, down to a value of 1.4±0.2 electrons per mol of protein, suggesting cluster loss upon repeated cycling. However, it is unlikely that [4Fe-4S] clusters were being converted into the [3Fe-4S] form, since no new waves were observed. The decrease in intensity is therefore more likely to be due to irreversible cluster loss.

To test the ease of convertibility of the [4Fe-4S] cluster to the 3Fe form, compared with native *Da* FdIII, the D14C solution potential was held at potentials ranging from −50 mV to +250 mV for 10 min. Under such conditions, the 8Fe form of *Da* FdIII is rapidly and totally converted into a 7Fe form as the 'labile' 4Fe cluster ($E_0' = -400$ mV) loses one Fe atom to give a [3Fe-4S]$^{1+/0}$ cluster ($E_0' = -140$ mV) [15]. However, we did not observe under such conditions any new waves, only a decrease in the 4Fe couple intensity. Cyclic voltammograms of the solution of D14C mutant incubated with ferricyanide showed a new redox couple ($E_0' = -125\pm10$ mV), which is again very close to the value of −140 mV observed for couple A of wild-type *Da* FdIII, and must correspond to the +1/0 couple of the [3Fe-4S] cluster.

Cluster transformation reactions are more easily followed electrochemically using the protein-film technique, because all the adsorbed protein molecules are under direct control of the applied potential [31]. The protein-film voltammogram of D14C *Da* FdIII (as isolated) is shown in Figure 9(a). One signal (pair of oxidation and reduction waves), B′, is detected at a potential ($E_0'$) of −450 mV, corresponding to the [4Fe-4S]$^{2+/1+}$ couple. Two minor signals, A′ and C′, are also observed ($E_{0,A'}' = -130$ mV, $E_{0,C'}' = -690$ mV at pH 7.5), and represent the [3Fe-4S]$^{1+/0}$ and [3Fe-4S]$^{0/2-}$ couples respectively. We have recently described the product of the two-electron couple, C′, the reduction wave of which is too drawn out to observe under these conditions of pH and scan rate [38]. Integration of the area under the oxidative waves A′ and C′ show that the [3Fe-4S] cluster population represents ≈ 5 % of the area under wave B (i.e ≈ 0.1 spin/mol for A′, considering B′ ≈ 2 spin/mol). Further cluster transformation was attempted by holding the potential at 0 mV for 1 min, but this only resulted in film loss. However, we obtained a significant proportion of [3Fe-4S] clusters by adding potassium ferricyanide to the electrolyte solution. The resulting voltammogram, after addition of 1.5 equiv. of Fe(CN)$_6$$^{3-}$, is shown in Figure 9(b). Signals A′ and C′ (oxidation) are now clearly discernable, and account for 25–30 % of the cluster population. Finally, the ferricyanide-oxidized film was transferred to a pot containing 1.5 equiv. of Fe(II) ions (Figure 9c). After cycling the potential, both waves, A′ and C′, decreased to less than 10 % of the total clusters. However, even after repeated cycling we could not obtain complete transformation of all the [3Fe-4S] cluster (Figure 9c). These results are in agreement with the spectroscopic results, which showed about 5 % [3Fe-4S] clusters (0.1 spin/mol) for the D14C samples after reconstitution, increasing to 30 % (0.6 spin/mol) upon incubation with ferricyanide and finally reverting to less than 10 % after reductive incubation with ferrous ions.

## DISCUSSION

The D14C mutant of *Da* FdIII has been overexpressed from a synthetic gene, using typical *E. coli* codon usage, cloned into the
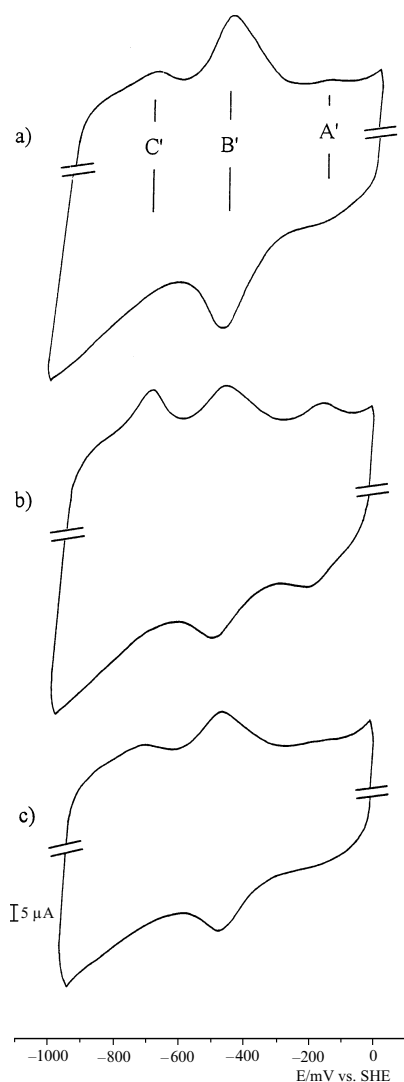
**Figure 9    Protein-film cyclic voltammetry of D14C *Da* FdIII**

(**a**) 138 $\mu$M Fd in 200 $\mu$M EGTA, 20 mM each Hepes, Mes and Taps, pH 7.6, 0.1 M NaCl and 2 mM neomycin ('mixed buffer'); (**b**) film transferred to mixed buffer + 200 $\mu$M ferricyanide; (**c**) film subsequently transferred to mixed buffer + 200 $\mu$M Fe(II). The scan rate was 500 mV·s$^{-1}$ and the temperature 4 °C

pET21d vector and transformed into *E. coli* strain BL21(DE3). The resulting polypeptide did not contain any iron–sulphur clusters. On the basis of our earlier work [24], in which the native sequence of *Da* FdIII was expressed also without cluster insertion, the polypeptide was partially purified and iron–sulphur clusters were inserted using standard reconstitution methods. The resulting protein was purified under anaerobic conditions. This protein has been shown by spectroscopic analysis to contain two [4Fe-4S]$^{2+/1+}$ clusters, both of which undergo a one-electron reduction at similar $E_0'$ values ($\approx -400$ mV). EPR spin quantification and variable temperature-MCD studies for the fully reduced sample show that it contains two [4Fe-4S]$^{1+}$ clusters, both having $S = 1/2$ with $g$-values of 2.059, 1.944 and 1.899. Spin–spin interaction between the two clusters is evident in the broadening and fine structure of the EPR spectrum. We conclude that two [4Fe-4S] clusters are present and that both are ligated by cysteines in the classic Fd fold.
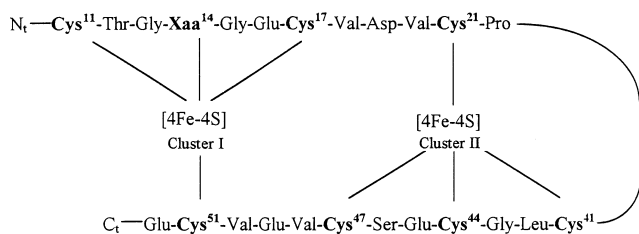
In the 8Fe form of native *Da* FdIII one [4Fe-4S]$^{1+}$ cluster has $S = 1/2$ and the other S = 3/2. The former spin belongs to the cluster which is inert to oxidation and co-ordinated by four cysteine residues, while the latter belongs to the oxidatively labile cluster which is bound by three cysteine residues and Asp$^{14}$ (or water). Hence the mutation D14C has changed the co-ordination to four cysteine residues, which is reflected in the switch of the ground state electronic spin from $S = 3/2$ to S = 1/2.

Using direct electrochemistry the protein shows a single reversible wave at a potential ($E_0'$) of $\approx -425$ mV, arising from both clusters. No electrochemical evidence for oxidative cluster transformation into a [3Fe-4S] form could be obtained even after holding the protein at potentials up to $+250$ mV for 10 min. This contrasts with the properties of the 8Fe native protein, which, under the same conditions, transforms rapidly and reversibly into a 7Fe form that contains a stable [3Fe-4S]$^{1+}$ cluster.

These results clearly show that the aspartate residue at position 14 is responsible for the facile metal exchange reaction at the [3Fe-4S] cluster in the native protein. Mutation of this ligand into a cysteine residue prevents the reversible loss of iron on mild oxidation. However, the clusters in D14C can be subjected to oxidative damage by the anaerobic addition of ferricyanide. Anaerobically reconstituted protein invariably contains 5–10 % of [3Fe-4S]$^{1+/0}$ clusters, as judged by EPR and electrochemistry. This signal was rapidly increased by addition of ferricyanide, but did not go to completion, as further cluster destruction occurred at higher ferricyanide concentration. After ferricyanide treatment the sample did show, in direct electrochemistry, a signal from the [3Fe-4S]$^{1+/0}$ couple with $E_0' = -130$ mV, the same as in the native 7Fe Fd. The reaction was reversible in the presence of Fe(II) ions and dithionite, or at low potential for the protein-film experiment, but a fraction of the [3Fe-4S] cluster population did not take up iron. This behaviour is rather characteristic of 8Fe Fds such as *Clostridium pasteurianum* (*Cp*) Fd, in which selective oxidation of one cluster to generate the [3Fe-4S] form is observed [39,40]. The 8Fe form of *Cp* Fd could only be recovered after incubation with Fe(II), dithionite and a reduced thiol such as dithiothreitol, followed by chromatographic purification.

We can now distinguish between two groups of 8Fe Fds, those with two [4Fe-4S(Cys)$_4$] clusters and those with [4Fe-4S(Cys)$_4$] and [4Fe-4S(Cys)$_3$(X)] [where Xaa = Asp or HO(H)]. The cluster which is co-ordinated closest to the N and C terminus, called cluster I (Scheme 1), is subject to reversible transformation when residue 14 is X or to more irreversible oxidative damage when residue 14 is cysteine. The second cluster, bound at the internal site, (cluster II) appears to be less susceptible to oxidative damage. Indeed, in other Fds, such as monocluster 4Fe or dicluster 7Fe, cluster II is either missing or replaced by a disulphide bridge (e.g. *D. gigas* FdII [41]), or has a particularly negative reduction potential (e.g. *Azotobacter vinelandii* FdI [42,42a]), implying that cluster I is most likely the physiological electron acceptor/donor.

The reactivity of cluster I may arise because of the exposure of one corner of the cubane to protein surface and hence to solvent. In the high-resolution X-ray structure of *C. acidi-urici* Fd [43], co-ordination of Cys$^{11}$ (equivalent to Asp$^{14}$ in *Da* FdIII) to the corner of cluster I shows an unusual Fe–S(Cys) bond angle and a lengthened Fe–S distance which may render it more labile. This suggests that in cluster I there is a distinct Fe site, Fe$_a$ (corresponding to Fe$_2$ in *C. acidi-urici* Fd structure) which can be lost to give a [3Fe-4S] cluster. Fe$_a$ is co-ordinated by Cys$^{11}$ in cysteine-only Fds and possibly by an aspartic acid in the aspartate Fds (D$^{14}$ in *Da* FdIII). These observations may account, at least in part, for the protein influence on the lability of the Fe$_a$ subsite,

N$_t$ —**Cys$^{11}$**-Thr-Gly-**Xaa$^{14}$**-Gly-Glu-**Cys$^{17}$**-Val-Asp-Val-**Cys$^{21}$**-Pro —

[4Fe-4S]  Cluster I          [4Fe-4S]  Cluster II

C$_t$ —Glu-**Cys$^{51}$**-Val-Glu-Val-**Cys$^{47}$**-Ser-Glu-**Cys$^{44}$**-Gly-Leu-**Cys$^{41}$**

**Scheme 1    Schematic representation of the ligands involved in Fe-S cluster binding in *Da* FdIII**

Wild-type: Xaa$^{14}$ = Asp; D14C, Xaa$^{14}$ = Cys.

such as that observed in the cysteine-only ligated cluster of *D. gigas* FdII.

However, our comparative studies of native and D14C *Da* FdIII show that it is the nature of the side chain, whether thiolate or carboxylate, which is crucial in allowing rapid and reversible metal exchange in *Da* FdIII, itself an intrinsic property of the [3Fe-4S]$^0$ cluster [16–19c,44]. Further evidence for aspartate ligation in the native 8Fe protein stems from our study of the pH-dependence of metal insertion in the [3Fe-4S] cluster of *Da* FdIII. It was shown that protonation of a group having a p$K$ of 5.5 competes with metal uptake (J. N. Butt, J. L. Breton, A. J. Thomson and F. A. Armstrong, unpublished work). This group has been tentatively assigned as Asp$^{14}$, although protonation of the cluster itself could not be ruled out. Thiolate (RS$^-$) is a stronger ligand for Fe(II) than carboxylate RCOO$^-$, and replacement of aspartate ligation by cysteine would therefore be expected to lead to a more inert [4Fe-4S] cluster. It should be noted also that the reduction potentials for the S-ligated (D14C) and O-ligated (native) [4Fe-4S] cluster of *Da* FdIII are very similar (Table 1). This suggests that the Fe subsite is, in both cases, co-ordinated by a protein-derived ligand which is negatively charged (-O$^-$) rather than neutral (-OH) in the native protein.

## REFERENCES

1    Beinert, H. (1990) FASEB J. **4**, 2483–2491
2    Johnson, M. K. (1994) Encycl. Inorg. Chem. **4**, 1896–1915
3    Liochev, S. I., Hausladen, A., Beyer, W. F. and Fridovich, I. (1994) Proc. Natl. Acad. U.S.A. **91**, 1328–1331
4    Cammack, R. (1992) Adv. Inorg. Chem. **38**, 281–322
5    Kennedy, M. C. and Stout, C. D. (1992) Adv. Inorg. Chem. **38**, 323–339
6    Klausner, R. D., Rouault, T. A. and Harford, J. B. (1993) Cell **72**, 19–28
7    Lazazzera, B. A., Beinert, H., Khoroshilova, N., Kennedy, M. C. and Kiley, P. J. (1996) J. Biol. Chem. **271**, 2761–2768
8    Bovier-Lapierre, G., Bruschi, M., Bonicel, J. and Hatchikian, E. C. (1987) Biochim. Biophys. Acta **913**, 20–26
9    Armstrong, F. A., George, S. J., Cammack, R., Hatchikian, E. C. and Thomson, A. J. (1989) Biochem. J. **264**, 265–273
10   Okawanara, N., Ogata, M., Yagi, T., Wakabayashi, S. and Matsubara, H. (1988) J. Biochem. (Tokyo) **104**, 196–199
11   Asso, M., Mbarki, O., Guigliarelli, B., Yagi, T. and Bertrand, P. (1995) Biochem. Biophys. Res. Commun. **211**, 198–204
12   Conover, R. C., Kowal, A. T., Fu, W., Park, J.-B., Aono, S., Adams, M. W. W. and Johnson, M. K. (1990) J. Biol. Chem. **265**, 8533–8541
13   Minami, Y., Wakabayashi, S., Wada, K., Matsubara, H., Kerscher, L. and Oesterhelt, D. (1985) J. Biochem. (Tokyo) **97**, 745–753.

14   Wakabayashi, S., Fujimoto, N., Wada, K., Matsubara, H., Kerscher, L. and Oesterhelt, D. (1983) FEBS Lett. **162**, 21–24
15   George, S. J., Armstrong, F. A., Hatchikian, E. C. and Thomson, A. J. (1989) Biochem. J. **264**, 275–284
16   Moura, I., Moura, J. J. G., Münck, E., Papaefthymiou, V. and LeGall, J. (1986) J. Am. Chem. Soc. **108**, 349–351
16a  Surerus, K. K., Münck, E., Moura, I., Moura, J. J. G. and LeGall, J. (1987) J. Am. Chem. Soc. **109**, 3805–3806
16b  Moreno, C, Macedo, A. L., Moura, I., LeGall, J. and Moura, J. J. G. (1994) J. Inorg. Biochem. **53**, 219–234
17   Butt, J. N., Armstrong, F. A., Breton, J., George, S. J., Thomson, A. J. and Hatchikian, E. C. (1991) J. Am. Chem. Soc. **113**, 6663–6670
17a  Butt, J. N., Sucheta, A., Armstrong, F. A., Breton, J., Thomson, A. J. and Hatchikian, E. C. (1991) J. Am. Chem. Soc. **113**, 8948–8950
17b  Butt, J. N., Niles, J., Armstrong, F. A., Breton, J. and Thomson, A. J. (1994) Nature Struct. Biol. **1**, 427–433.
18   Reference deleted
19   Conover, R. C., Park, J.-B., Adams, M. W. W. and Johnson, M. K. (1990) J. Am. Chem. Soc. **112**, 4562–4564
19a  Srivastava, K., Surerus, K. K., Conover, R. C., Johnson, M. K., Park, J.-B., Adans, M. W. W. and Münck, E (1993) Inorg. Chem. **32**, 927–936
19b  Fu, W., Telser, J., Hoffman, B. M., Smith, E. T., Adams, M. W. W., Finnegan, M. G., Conover, R. C. and Johnson, M. K. (1994) J. Am. Chem. Soc. **116**, 5722–5729
19c  Finnegan, M. G., Conover, R. C., Park, J.-B, Zhou, Z. H., Adams, M. W. W. and Johnson, M. K. (1995) Inorg. Chem. **34**, 5358–5369
20   Calzolai, L., Gorst, C. M., Zhao, Z.-H., Teng, Q., Adams, M. W. W. and La Mar, G. N. (1995) Biochemistry **34**, 11373–11384
21   Butt, J. N., Sucheta, A., Armstrong, F. A., Breton, J., Thomson, A. J. and Hatchikian, E. C. (1993) J. Am. Chem. Soc. **115**, 1413–1421
22   Werst, M. M., Kennedy, M. C., Beinert, H. and Hoffman, B. M. (1990) Biochemistry **29**, 10528–10532
23   Moura, J. J. G., Moura, I., Kent, T. A., Lipscomb, J. D., Huynh, B. H., LeGall, J., Xavier, A. V. and Münck, E. (1982) J. Biol. Chem. **257**, 6259–6267
24   Busch, J. L. H., Breton, J. L. J., Bartlett, B. M., James, R., Hatchikian, E. C. and Thomson, A. J. (1996) Biochem. J. **314**, 63–71
25   Curtis, M. D. and James, R. (1991) Mol. Microbiol. **5**, 2727–2733
26   Maniatis, T. E., Fritsch, F. and Sambrook, J. (1982) Molecular Cloning: A Laboratory Manual, Cold Spring Harbor Laboratory Press, Cold Spring Harbor, NY
27   Laemmli, U. K. (1970) Nature (London) **227**, 680–685
28   Lowry, O. H., Rosebrough, N. J., Farr, A. L. and Randall, R. J. (1951) J. Biol. Chem. **193**, 265–275
29   Aasa, R. and Vänngård, T. (1975) J. Magn. Reson. **19**, 308–315
30   Cheesman, M. R., George, S. J. and Thomson, A. J. (1993) Methods Enzymol. **226**, 199–231
31   Armstrong, F. A., Butt, J. N. and Sucheta, A. (1993) Methods Enzymol. **227**, 479–500
32   Davy, S. L., Breton, J., Osborne, M. J., Thomson, A. J., Thurgood, A. P., Lian, L. Y., Pétillot, Y., Hatchikian, E. C. and Moore, G. R. (1994) Biochim. Biophys. Acta **1209**, 33–39
33   Beinert, H. and Thomson, A. J. (1983) Arch. Biochem. Biophys. **222**, 333–361
34   Hatchikian, E. C., Cammack, R., Patil, D. S., Robinson, A. E., Richards, A. J. M., George, S. J. and Thomson, A. J. (1984) Biochim. Biophys. Acta **784**, 40–47
35   Mathews, R., Charlton, S., Sands, R. and Palmer, G. (1974) J. Biol. Chem. **249**, 4326–4328
36   Johnson, M. K., Robinson, A. E. and Thomson, A. J. in Iron–Sulfur Proteins, vol. 4, (Spiro, T. G., ed.),   pp. 368–406, Academic Press, New York
37   Bard, A. J. and Faulkner, L. R. (1980) Electrochemical Methods, Fundamentals and Applications pp. 213–248,   Wiley, New York
38   Duff, J. L. C., Breton, J. L. J., Butt, J. N., Armstrong, F. A. and Thomson, A. J. (1996) J. Am. Chem. Soc., **118**, 8593–8603
39   Thomson, A. J., Robinson, A. E., Johnson, M. K., Cammack, R., Rao, K. K. and Hall, D. O. (1981) Biochim. Biophys. Acta **637**, 423–432
40   Bertini, I., Briganti, F., Calzolai, L., Messori, L. and Scozzafava, A. (1993) FEBS Lett. **332**, 268–272
41   Kissinger, C. R., Sieker, L. C., Adman, E. T. and Jensen, L. H. (1991) J. Mol. Biol. **219**, 693–715
42   Stout, C. D. (1989) J. Mol. Biol. **205**, 545–555
42a  Stout, G. H., Turley, S., Sieker, L. C. and Jensen, L. H. (1988) Proc. Natl. Acad. U.S.A. **85**, 1020–1022
43   Duée, E. D., Fanchon, E., Vicat, J., Sieker, L. C., Meyer, J. and Moulis, J.-M. (1994) J. Mol. Biol. **243**, 683–695
44   Zhou, J., Hu, Z., Münck, E. and Holm, R. H. (1996) J. Am. Chem. Soc. **118**, 1966–1980